International Journal of Technology 15(5) 1218-1236 (2024)
Received March 2024 / Revised April 2024 / Accepted May 2024

International Journal of Technology

http://ijtech.eng.ui.ac.id

Membrane Air Separation Process Simulation: Insight in Modelling Approach Based on Ideal and Mixed Permeance Values

Sergey Kryuchkov[1*], Kirill Smorodin[1], Anna Stepakova[1], Artem Atlaskin[1], Nikita Tsivkovsky[1], Maria Atlaskina[1], Maria Tolmacheva[1], Olga Kazarina[2], Anton Petukhov[2], Andrey Vorotyntsev[2], Ilya Vorotyntsev[1]

[1]*Laboratory of SMART Polymeric Materials and Technologies, Mendeleev University of Chemical Technology of Russia, Miusskaya square, 9, Moscow, 125047 Russia*
[2]*Chemical Engineering Laboratory, Lobachevsky State University of Nizhny Novgorod, 23 Gagarin Avenue, Nizhny Novgorod, 603022, Russia*

Abstract. The presented work aims to study the gas transport characteristics of polymeric hollow-fiber gas separation membranes. The study focused on examining the gas transport characteristics of polymeric hollow-fiber gas separation membranes using materials such as polysulfone (PSF), polyphenylene oxide (PPO), polyetherimide (PEI), and polyetherimide with polyimide (PEI+PI) for the separation of air mixtures. The permeance values of pure gases O2 and N2and the mixed permeances of oxygen and nitrogen during air separation were obtained. Membrane permeance was measured using an analytical setup combined with a mass spectrometer on membrane modules with different effective membrane areas. Mathematical models of the gas separation process built because of these values show significant discrepancies. To obtain a gas mixture with 95 mol.% nitrogen from the air, considering the mixture permeance, 15.8% more PSF membrane area is required than considering the permeance of pure gases. For a PPO membrane, this value is 13.9%; for PEI, 19.8% less area is required, and for PEI+PI, 15.9% less. In the design of industrial or semi-industrial membrane installations, such discrepancies can lead to significant technical and economic errors.

Keywords: Air mixture separation; Membrane gas separation; Mixture permeance; Process modeling

1. Introduction

Air separation is one of the main sources of nitrogen and oxygen for chemical technology (Cheun *et al.,* 2023; Kianfar and Cao, 2021; Krzystowczyk *et al.,* 2021). Manufacturers use pure nitrogen as a raw material to produce ammonia and nitrogen fertilizers in the oil and gas industry and to create an inert environment in various chemical industry processes. Petrochemical processes, the oxygen conversion of methane, metallurgy, medicine, and rocket fuel all utilize oxygen. The cost of pure gases (with a concentration of > 95 vol.%) is typically comprised of the cost of acquisition and purification. However, in the case of oxygen and nitrogen, as they can be obtained from air, their cost is solely determined by the expense of their separation. Consequently, the cheaper

*Corresponding author's email: kriuchkov.s.s@muctr.ru, Tel.: +7 (999) 138-95-43
doi: 10.14716/ijtech.v15i5.6987

their separation, the more affordable the gases become and, with it, all the products manufactured using them.

There are currently three main methods of air separation used in industry: cryogenic distillation, adsorption, and membrane gas separation. Cryogenic air separation is the most widespread method, which allows the separation of air by components with high-purity products (Cheng *et al.,* 2021; Young *et al.,* 2021; Zhou *et al.,* 2021). The disadvantage of this method is the high energy intensity of the process, which is caused by the need to maintain low temperatures (up to -200 ˚C), which makes the process economically feasible only in case of application of the method within the framework of large-capacity production. Adsorption method – pressure swing adsorption (PSA) is effective for medium tonnage production and processes (Kamin, Bahrun, and Bono, 2022; Tian *et al.,* 2022). Membrane technology is characterized by high energy efficiency and produces nitrogen with a concentration of > 99 vol.% (Liu *et al.,* 2023; Chuah, Goh, and Bae, 2021; Tu and Zeng, 2021; Fujikawa, Selyanchyn, and Kunitake, 2020).

Membrane technology is currently a source of profound interest, especially in the context of green chemistry. This is primarily due to the energy efficiency and environmental sustainability of membrane units. Membrane units are able to purify gases under ambient conditions, without phase transformations and without the supply or removal of thermal energy. Moreover, while cryogenic and adsorption methods of air separation have limitations in terms of economic feasibility in relation to the scale of production, membrane technology can be easily scaled up and applied in the largest plants as well as in the smallest ones (Bera, Godhaniya, and Kothari, 2022; Petukhov *et al.,* 2022, 2021; Valappil, Ghasem, and Al-Marzouqi, 2021; Atlaskin *et al.,* 2020; 2019; Vorotyntsev *et al.,* 2006). Also, trace amounts of impurities formed as a result of human activity may be present in the air. For example, NOx or SO_2 removal is possible using membrane technology (Kartohardjono *et al.,* 2024; 2023; Karamah *et al.,* 2021).

Speaking of chemical technology in general, one of the key methods for designing any industrial installation today is mathematical modeling (Bittner *et al.,* 2023; Ilyushin and Kapostey, 2023; Mayer and Gróf, 2020; Trubyanov *et al.,* 2019). However, the effectiveness of the application of mathematical modeling is, to a marked extent, limited by the quality of the models used. In the context of membrane technology, the application of ideal permeances of gas mixture components significantly affects the quality of calculations. This can lead to both excessive and insufficient parameters of the membrane unit required to achieve the gas separation goal.

The gas transport characteristics of a number of polymer gas separation membrane materials selected for the experiment were taken from published papers (Table 1). The membrane materials considered in this study, polysulfone (PSF), polyphenylene oxide (PPO), and polyetherimide (PEI), were selected to analyze the literature data on gas transport performance studies. The table is divided into two parts: the first part of the table shows the permeability coefficients (P) in Barrers, while the second part of the table shows the permeance (Q) in GPU. The permeance values expressed in GPU (Gas Permeation Unit) characterize the membrane unit to a greater extent. The permeability coefficient expressed in Barrers is dependent on the thickness of the membrane selective layer and characterizes the membrane material to a greater extent. It should be noted that at a membrane selective layer thickness of 1 μm, 1 GPU is equivalent to 1 Barrer. Given that not all works specify the thickness of the selective layer, it is not possible to compare permeance with permeability coefficients. At the same time, the selectivity value is a dimensionless value and can be included in the comparison, regardless of whether the value was obtained through the ratio of permeances or through the ratio of permeability coefficients.

Table 1 Gas transport characteristics of polymeric gas separation membranes

Membrane	P_{O2}, barrer[a]	P_{N2}, barrer[a]	Selectivity, $\alpha(O_2/N_2)$	T, °C	Pressure Difference, bar	Ref.
PSF	1.05	0.165	6.4	24	3.5	(Pfromm *et al.,* 1993)
	1.29	0.22	5.9	35	10	
	1.5	0.26	5.8	35	2	(Reid *et al.,* 2001)
	1.1	0.23	4.8	30	1	(Ng *et al.,* 2004)
	1.06	0.171	6.2	25	3.5	(Pinnau and Koros, 1991)
	1.2	0.2	6	35	5	(Barbari, Koros, and Paul, 1989)
PPO	17	3.62	4.7	35	2	(Wright and Paul, 1998)
	17	4.47	3.8	30	1	(Polotskaya *et al.,* 1996)
	19.08	4.65	4.1	30	1	(Polotskaya *et al.,* 2007)
PEI	0.32	0.05	6.4	22	0.2-0.9	(Checchetto *et al.,* 2022)
	0.4	0.05	7.6	35	5	(Barbari, Koros, and Paul, 1989)
	0.38	0.054	7.1	35	3.5	(Hao, Li, Chung, and 2014)
	0.4	0.05	8	35	10	(Chen, Kaliaguine, and Rodrigue, 2019)
Membrane	Q_{O2}, GPU[b]	Q_{N2}, GPU[b]	Selectivity, $\alpha(O_2/N_2)$	T, °C	Pressure Difference, bar	Ref.
PSF	27.5	4	6.9	24	3.5	(Pfromm *et al.,* 1993)
	13.6	2.88	4.8	30	1	(Ng *et al.,* 2004)
	39.3	6.3	6.2	25	3.5	(Pinnau and Koros, 1991)
PPO	40	10	4	22.5	5	(Chenar *et al.,* 2006)
	20	4.8	4.1	35	4	(Visser, Masetto, and Wessling, 2007)
PEI	2.89	0.33	8.8	30	2	(Chen, Kaliaguine, and Rodrigue, 2019)
	11.5	1.77	6.5	27	6	(Ekiner and Kulkami, 2003)
	2.6	0.63	4.1	22	6.9	(Saimani *et al.,* 2011)

[a]1 Barrer = 1×10^{-10} $cm^3(STP) \cdot cm \cdot cm^{-2} \cdot s^{-1} \cdot cmHg^{-1}$
[b]1 GPU = 1×10^{-6} $cm^3(STP) \cdot cm^{-2} \cdot s^{-1} \cdot cmHg^{-1}$

Data on the permeabilities of isotropic polysulfone films and asymmetric membranes are presented in (Pfromm *et al.,* 1993). An asymmetric membrane with a selective layer thickness of 80 nm, prepared using variable-pressure constant-volume technique, showed an O_2/N_2 selectivity of 6.4. Also, temperature and pressure dependences of permeability coefficients, as well as the influence of CO_2 additives on the separation process, are presented. It is shown that with increasing temperature, the flows increase and selectivity decreases. The O_2/N_2 pair selectivity for pure PSF in (Reid *et al.,* 2001) was 5.8, which is similar to the data presented in (Pfromm *et al.,* 1993). Ng *et al.* (2004) conducted a study on ten PSF membranes (Ng *et al.,* 2004). Table 1 summarizes the average values and converts the permeance from GPU to Barrer, taking into account the selective layer thickness reported in the paper. Pinnau and Koros (1991) conducted research on the methods of molding polysulfone membrane films. The values in Table 1 are based on the dry/wet phase inversion method, which the authors claim to be optimal. In a study by (Barbari, Koros, and Paul, 1989), the gas transport characteristics of commercially available bisphenol-A polymer membranes were investigated. The results include data for various types of membranes, such as polycarbonate, polysulfone, polyacrylate, polyetherimide, and polyhydroxyether. Among these, PEI membranes exhibit the highest selectivity for the O_2/N_2 pair, although their oxygen permeability coefficient is three times lower than that of polysulfone films.

Wright and Paul (1998) investigated the gas transport properties of polyphenylene oxide films under UV irradiation, such as permeability, diffusion, and sorption coefficients.

Increasing the exposure time and intensity of UV irradiation resulted in a decrease in permeability coefficient and a significant increase in selectivity. The addition of benzophenone did not significantly change the gas transport properties of the film. Table 1 shows the values for pure polyphenylene oxide without UV irradiation and without the addition of benzophenone.

The influence of polyphenylene oxide's molecular weight on membranes' gas transport properties was studied by (Polotskaya *et al.,* 1996). It was found that it is possible to obtain composite membranes with the same transport properties from polymers with different values of molecular weight under the condition [n] · c = const. In (Polotskaya *et al.,* 2007), the authors studied homogeneous membranes from a fullerene-polyphenylene oxide composite with fullerene content of 1-2 wt.%. The addition of 1% fullerene increased the O_2/N_2 selectivity from 4.1 to 4.5, reducing the oxygen permeation coefficient by 0.95 barrer (to 18.13 barrer). Further increase in fullerene concentration leads to a small increase in selectivity (up to 4.6) and a significant decrease in permeability coefficient (up to 15.12 barrer).

Checchetto *et al.* (2022) conducted a study on the gas transport characteristics of membranes made of polyimide (Matrimid®), polyetherimide (PEI), and poly lactic acid (PLA) (Checchetto *et al.,* 2022). Their research focused on the separation of a gas mixture with the inclusion of CO and CO2. The researchers obtained characteristics for both individual gases and components of the gas mixture using a mass spectrometric apparatus. The discrepancy in the results is due to the errors of the analysis. Also, diffusion coefficients are given in the paper.

Polymer films from polyetherimide (Ultem® 1010) and Ultem/PIM-1 (polymer of intrinsic microporosity) mixture with different concentrations were studied (Hao, Li, Chung, and 2014). Permeability coefficients were obtained for individual gases and for components of CO_2/CH_4 and CO_2/N_2 gas mixtures. The authors observed that the selectivities of the gas mixtures were higher than the ideal selectivities for pure gas pairs due to the affinity of PIM-1 for CO_2 and its better competitive sorption. The same phenomenon was observed in (Du *et al.,* 2012; Thomas *et al.,* 2009).

Chen, Kaliaguine, and Rodrigue (2019) investigated asymmetric hollow fiber membranes fabricated by phase inversion using commercially available polymers, including polyethersulfone (PES), polyetherimide (Ultem® 1000), and polyimides (Matrimid® 5218) (Chen, Kaliaguine, and Rodrigue, 2019). Hollow-fiber membranes and films were fabricated. The values given in barrers in Table 1 correspond to the parameters of the polyetherimide membrane film, while the values in GPU are given for the PEI hollow fiber membrane. Taking into account the thickness of the selective layer specified in the article, which is equal to 150 nm, when converting from GPU to barrer, the values of permeability coefficients for films and hollow-fiber membranes are equal. The PPO hollow fiber membranes show a stable O_2/N_2 selectivity of about 4. In (Chenar *et al.,* 2006), the authors concluded that PPO membranes showed stable permeance when the permeance of polyimide membranes decreased after three months of operation. The work by (Visser, Masetto, and Wessling, 2007) confirms that PPO membranes are not very susceptible to plasticization when separating CO_2/CH_4 mixtures due to the strong competitive sorption effects.

Ekiner and Kulkarni describe a method for producing mixed matrix hollow fiber membranes in their patent (Ekiner and Kulkami, 2003). The Ultem® 1000 polyetherimide membranes exhibit O_2 permeances ranging from 7.2 to 13.7 GPU and O_2/N_2 selectivities ranging from 6.1 to 7.3. These values depend on the wind-up rate and draw ratio. The films

obtained from Ultem® 1000 polyetherimide using the technology described in (Saimani *et al.,* 2011) showed similar permeance values, but the selectivity is much lower.

This work is devoted to studying the influence of the method of measuring membrane permeance on the results of mathematical modeling of the process of membrane gas separation using the example of an air mixture. To do this, we measured the permeance of commercially available hollow fiber membranes for nitrogen and oxygen for individual gases and components of the air mixture. The obtained permeance values were used to construct a mathematical model of a membrane gas separation unit in the Aspen Plus environment. Then, in the model, the effective membrane area was gradually increased, and changes in the concentration of components in the streams were monitored. The plotted dependences of the concentration of components on the effective membrane area were supplemented with experimental data obtained during air separation on membrane modules with different effective membrane areas. The result of comparing the two curves obtained is the difference in effective membrane areas required to obtain 95 mol.% nitrogen in the retentate stream and 40 mol.% oxygen in the permeate stream. The resulting difference was expressed as a percentage of the calculated effective membrane area obtained using the membrane permeabilities for individual gases. Such deviations ranged from 13.9% to 15.9% for nitrogen and from 6.7% to 29.2% for oxygen, which literally demonstrates by how many percent the number of membranes must be increased or decreased to achieve the required concentrations. Thus, using ideal characteristics when calculating a mathematical model for industrial application planning may lead to significant errors and losses in CAPEX and OPEX. Errors in calculating the required effective membrane area lead to several problems at once: unnecessary or unexpected costs for membrane elements, gas lines, compressor stations, and more. Considering that the greatest contribution to production costs is made by the energy of the process, compression, and evacuation, an error in calculating the required power of the station will lead to significant additional costs.

2. Methods

The study of gas transport characteristics was carried out on polymeric hollow-fiber gas separation membranes based on polysulfone (PSF), polyphenylene oxide (PPO), polyetherimide (PEI), polyetherimide with polyimide (PEI+PI) purchased from Hangzhou Kelin Aier Qiyuan Equipment Co., Ltd. (Hangzhou, China). For the study of permeances for individual gases, the main components of the air-gas mixture were used: pure gases N_2 (99.9995 vol.%), O_2 (99.99 vol.%). He (99.9999 vol.%) and Ar (99.999 vol.%), purchased from NII KM (Russia, Moscow), were used as carrier gases in the membrane modules and for purging the experimental setup.

2.1. Study of Individual and Mixture Permeance

To study permeance, membrane cells were fabricated from tubes with an outer diameter of 1/4" made of stainless steel of the S316 brand (Hy-Lok, Korea), 16 cm long, with 40 hollow-fiber membranes placed inside. Photographs of the membrane module are presented in Figure 1.

Figure 1 A membrane module for studying the gas transport characteristics of hollow-fiber gas separation membranes

The experimental setup included gas flow controllers, a mixing chamber, a vacuum pumping post, and a mass spectrometer used to study the hollow-fiber membrane modules. The experimental setup's principle scheme is shown in Figure 2.

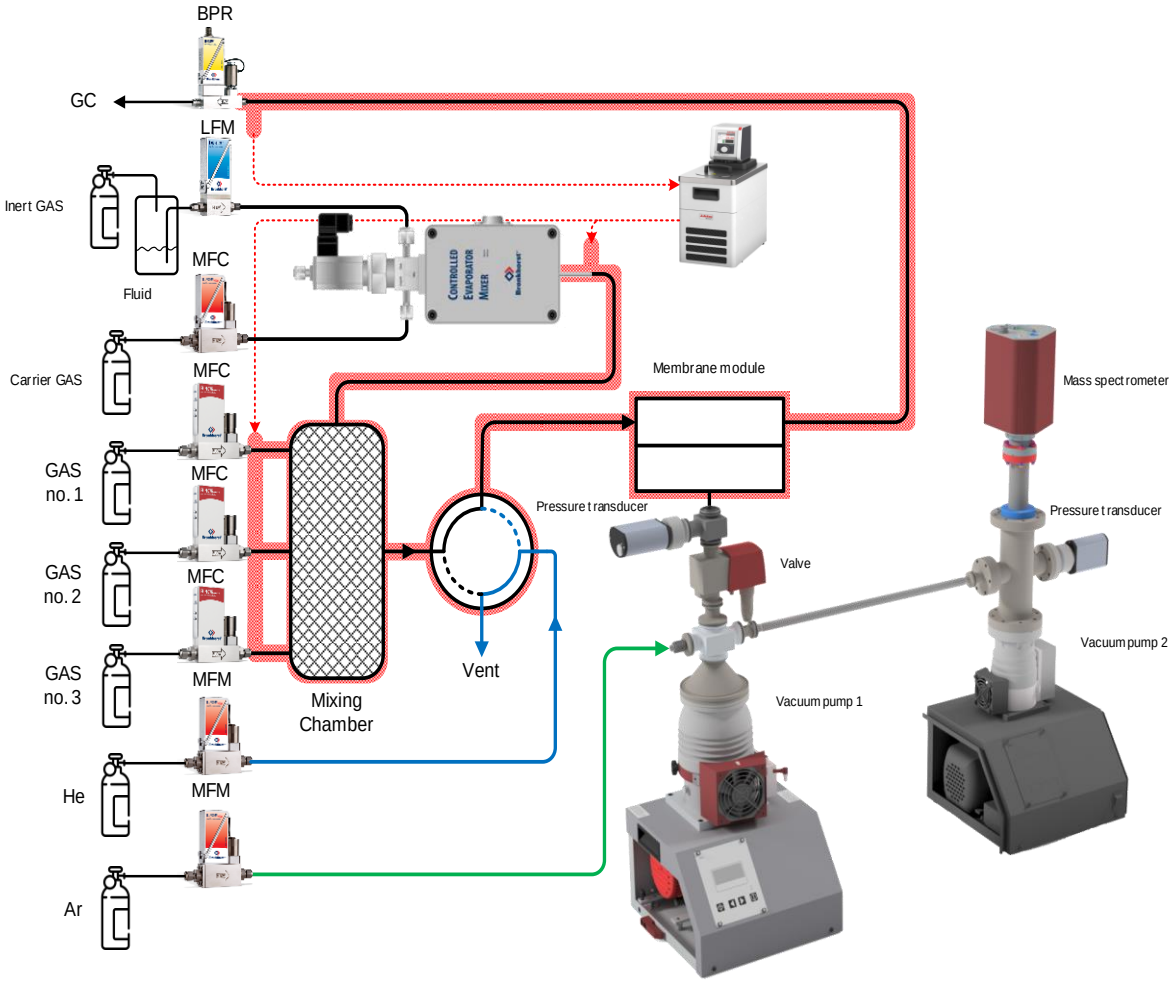

Figure 2 Schematic diagram of the setup for determination of gas transport characteristics of a membrane with a mass spectrometer

The gas distribution system includes five mass flow controllers (Bronkhorst FG-201CV, Bronkhorst F201CV, Bronkhorst F201CM), a back-pressure regulator “before itself” (Bronkhorst P702CM), a four-port two-position valve, vacuum pump 1 (Pfeiffer Hi-Cube ECO 300), vacuum pump 2 (Pfeiffer Hi-Cube 80 Eco). Three Bronkhorst FG-201CV regulators served to supply gas to the mixing chamber. With their help, you can supply both pure gas and, by dynamically mixing the flows in the mixing chamber, you can create a three-component gas mixture with specified concentrations. Other mass flow controllers

are used to supply argon and helium to the system. The back-pressure regulator maintains the set pressure in the high-pressure cavity A four-port two-position valve is used to receive two gas flows. The first input receives either the gas being tested or a gas mixture from the mixing chamber, while helium is introduced through the second input. Depending on the valve's position, one of the flows enters the ventilation system, while the other flows into the high-pressure cavity of the membrane module. A vacuum pump, labeled as Vacuum Pump 1, creates a vacuum in the low-pressure cavity of the membrane module. The mass spectrometer chamber maintains a high vacuum level with vacuum pump 2. Vacuum pumps comprise membrane and turbo-molecular pumps.

The main component of the analytical stand is a mass spectrometer (Pfeiffer PrismaPro QMG 250 M2). A pressure transducer (Pfeiffer MPT200) records the vacuum level. The stand is equipped with a membrane valve with an electromagnetic drive (Pfeiffer DVC 025 PX) that disconnects the vacuum equipment from the gas distribution system in case of membrane damage and a sharp increase in pressure in the low-pressure cavity.

The procedure for studying gas transport characteristics includes the following steps. The gas flow regulator supplies helium, which is directed to a four-port valve with a constant flow of 50-150 cm^3/min. The valve is switched to a position that connects the helium flow to the high-pressure cavity of the membrane module for purging. At the same time, the analyzed pure gas or gas mixture enters the mixing chamber. Argon is supplied directly to the analytical unit with a constant flow of 4 cm^3/min to calibrate the mass spectrometer to calculate gas flows depending on the output signal. The system purges with helium until it removes impurity components, which are monitored in real time using the mass spectrum. The mass spectrometer delay is 1 ms.

The two-position valve switches (switching time 8 ms) to a position in which the gas flow under study from the mixing chamber is directed into the high-pressure cavity of the membrane module. The pressure in the supra-membrane space and the adjustment of the flows of each gas were carried out in the FlowPlot program. Pressure in the submembrane space and the mass spectrometer chamber was monitored using PV TurboViewer software, and the mass spectrum was displayed and recorded in PV MassSpec software.

Membrane permeances were calculated using the formula (see equation 1):

$$Q = \frac{J_i}{\Delta p \cdot A}, \frac{cm^3(STP)}{cm^2\ s\ cmHG} \quad (1)$$

where J_i is the volumetric flow rate of the component i in the permeate, cm^3/s; Δp is the difference in the partial gas pressures through the membrane, cmHg; and A is the area of the membrane, cm^2. The software of the mass spectrometer made it possible to transform the signal with respect to each component under determination into the value of its partial pressure.

Therefore, the volumetric flow rate of the permeate can be determined by the formula (see equation 2):

$$\frac{J_i}{J_{Ar}} = \frac{p_i}{p_{Ar}} \quad (2)$$

where J_{Ar} is the volumetric flow rate of argon, cm^3/min; p_i is the partial pressure of the component i in the permeate, mmHg; and p_{Ar} is the partial pressure of argon in the permeate, mmHg.

The formula (see equation 3) calculated the selectivity for the gas pairs:

$$\alpha_{A/B} = \frac{Q_A}{Q_B} \quad (3)$$

where Q_A is the permeance of component A, and Q_B is the permeance of component B.

2.2. Membrane Separation Unit Simulation

To perform a simulation study of the membrane gas separation process using the Aspen Plus environment (Bedford, MA, USA), we used a custom ACM user block. That block is an updated version of the hollow fiber membrane element, which was developed by Ajayi and Bhattacharyya during the DOE Carbon Capture Simulation Initiative (CCSI) ("GitHub—CCSI-Toolset/Membrane_Model: Membrane Separation Model: Updated Hollow Fiber Membrane Model and System Example For Carbon Capture. Available online: https://github.com/CCSI-Toolset/membrane_model (accessed on 15 December 2023)," n.d.). This one-dimensional partial differential equation (PDE)--based multi-component can apply to materials where permeation occurs according to the solution-diffusion mechanism. Here, gas permeances are independent of the pressures, concentrations, and stage cut. The separation process occurs under isothermal conditions. That model allows us to predict the value of the pressure drop along the fiber bore side and the shell side of a unit under the Hagen–Poiseuille equation for a compressible fluid. In this model, the gas mixture feeds the unit from the shell side of the hollow fibers and permeates to the fiber bore. In a steady-state mode, the membrane module operates by utilizing countercurrent flows. The model assumes ideal gas mixture behavior and provides a profile of the component fluxes and concentrations. Depending on the variables specified, the user can perform rating or design calculations using the equation-oriented structure to satisfy the degrees of freedom.

2.3. Experimental Implementation of the Gas Separation Process

Experiments on the separation of the air-gas mixture were carried out on membrane modules with different effective membrane areas. When the effective membrane area increases, taking into account that the feed gas flow does not change, there is a consistent increase in the permeate flow and stage-cut value (see equation 4):

$$\theta = \frac{l_{perm}}{l_{feed}}, \quad (4)$$

where l_{perm} – volume permeate flow ($cm^3\ min^{-1}$), l_{feed} – volume feed flow ($cm^3\ min^{-1}$).

Modules with a small number of hollow fiber membranes (40, 45, 50, 55, 60 fibers) were fabricated. Modules with known effective membrane areas were also used: for PSF, PPO, PEI – 1000 cm^2, 2500 cm^2, 5000 cm^2, for PEI+PI – 100 cm^2, 200 cm^2 and 300 cm^2.

During the separation of an air-gas mixture from an air compressor, the researchers conducted the experiment. The feed gas mixture stream entered the membrane module with a defined flow rate, which was constant for each type of membrane and was maintained by a gas flow controller. The permeate stream was analyzed using a mass spectrometer; the retentate stream was analyzed by gas chromatography (GC) GC-1000 (Chromos Ltd, Russia) equipped with a thermal conductivity detector (TCD).

3. Results and Discussion

3.1. Gas Transport Characteristics Study by Individual Components

Results should be presented clearly and concisely, focusing on the most significant or main findings of the research. The discussion must explore the significance of the results. Provide an adequate discussion or comparison of the current results with similar findings in previously published articles to demonstrate the positioning of the present research (if available). To study the gas transport characteristics, membrane cells were fabricated, separately with each of the membranes under investigation. The gas transport characterization unit, equipped with a mass spectrometer, is used to calculate the permeate stream value for each gas. Given a known flow value, effective membrane area, and pressure

difference, the gas permeance is calculated and measured in GPU. This value allows the gas transport characteristics to be compared without dependence on the selective layer thickness. The results of the measurements are presented in Table 2.

Table 2 Permeance of individual gases for the investigated hollow fiber gas separation membranes

Membrane	Q, GPU*		α_{O_2/N_2}
	O_2	N_2	
PSF	51.4	12.8	4.02
PPO	47.9	9.40	5.1
PEI	3.45	0.58	6.0
PEI+PI	6.65	1.68	3.96

*1 GPU = 1×10^{-6} $cm^3(STP) \cdot cm^{-2} \cdot s^{-1} \cdot smHg^{-1}$

3.2. Mixture Permeance Study

The study of mixture permeance was carried out on a real air mixture supplied by the compressor to the measuring unit. As a result, the values of the flows of the components of the air mixture entering the submembrane space were obtained. The data of the experiment are given in Table 3. As shown in the table, the materials of the studied membranes can be arranged in the following order based on permeance value: PEI < PEI+PI < PPO < PSF. Similarly, the values of selectivity for the gas vapor O2/N2 can be arranged as follows: PEI+PI < PSF < PPO < PEI. The experimental results allow us to divide the materials into two pairs. The first pair is PSF and PPO, which, when the object of study was changed from individual components to a real air-gas mixture, showed a decrease in oxygen permeance, an increase in nitrogen permeance, and, as a consequence, a decrease in selectivity. The second pair is PEI and PEI+PI membranes, which show an increase in selectivity due to increased permeabilities, which are more for oxygen and less for nitrogen.

Table 3 Permeance of gas mixture components for the investigated hollow fiber gas separation membranes

Membrane	Q, GPU*		α_{O_2/N_2}
	O_2	N_2	
PSF	44.12	13.25	3.33
PPO	41.53	9.40	4.42
PEI	4.33	0.66	6.59
PEI+PI	7.69	1.86	4.15

*1 GPU = 1×10^{-6} $cm^3(STP) \cdot cm^{-2} \cdot s^{-1} \cdot smHg^{-1}$

3.3. Comparison of Study Methods for Gas Transport Characteristics

For modeling technological processes of gas separation using the Aspen Plus environment (Bedford, MA, USA), a custom ACM user block was used. Using gas transport characteristics obtained by analysis of permeances of pure gases and permeances of gas mixture components, the process of air gas separation is modeled. In this study, the result of the process modeling is presented as a dependence of nitrogen and oxygen concentrations in the retentate and permeate streams, respectively, on the effective membrane area. The modeled curves are supplemented with experimental values obtained during the separation of a real air-gas mixture. The dependences of the modeled straight lines and experimental points for membrane modules with 40, 45, 50, 55, and 60 hollow-fiber membranes are shown in Figures 5-8.

Figures 3 and 4 confirm the tendencies described in Section 3.2. The concentrations of nitrogen in the retentate stream and oxygen in the permeate stream are lower for the

separation of the real air mixture compared to the results of the pure gas permeance model. The polysulfone hollow fiber membrane has lower selectivity than the polyphenylene oxide membrane, which is why the component concentrations for PPO are higher. The membrane module model with 40 polysulfone hollow-fiber membranes has an effective area of 60 cm^2. The calculated oxygen concentration (Figure 3) was 45.55 mol.% based on the modeling results for the permeances of the components of the real air mixture and 50.13 mol.% based on the modeling results for the permeances of pure gases. For nitrogen, these values are 79.26 mol.% and 79.32 mol.%, respectively. The concentration of nitrogen in the modeling of air-gas mixture separation on 40 hollow polyphenylene oxide fibers (Figure 4) is 79.48 mol.% and 79.57 mol.% according to the results of modeling by individual permeances. For oxygen, these values are 52.8 mol.% and 56.1 mol.%, respectively. The effective area of such a membrane module is 112.6 cm^2.

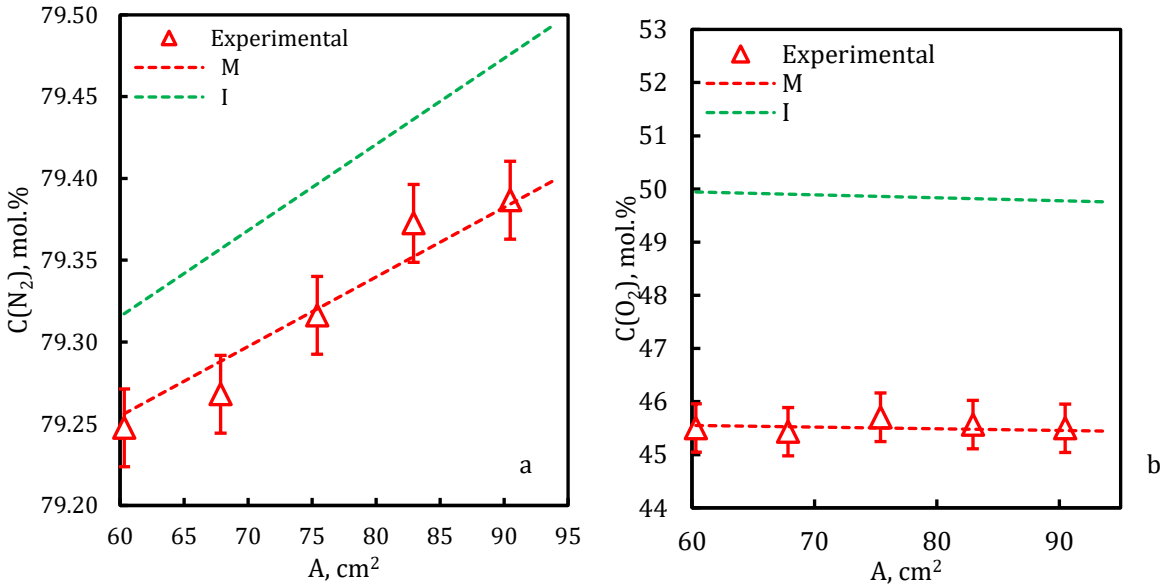

Figure 3 Dependence of concentration (a - N_2 in retentate stream; b - O_2 in permeate stream) on the effective area of PSF membrane. Experimental - experimentally obtained concentrations of components; M - line obtained by modeling of the gas separation process taking into account the mixture gas transport characteristics; I - line obtained by modeling of the gas separation process considering the gas transport characteristics of individual components

At a separation of air-gas mixture on hollow-fiber membranes from polyetherimide (Figure 5) and polyetherimide with polyimide (Figure 6), there is an inverse dependence - concentrations of components at the output of modules are higher than the calculated line on permeances of pure gases, selectivity on the real gas mixture is higher. The calculated concentration of oxygen (Figure 5) was 62.79 mol.% according to the results of modeling by permeances of components of real air mixture and 60.72 mol.% according to the results of modeling by permeances of pure gases. For nitrogen, these values are 79.21 mol.% and 79.16 mol.%, respectively. The concentration of nitrogen at the modeling of air-gas mixture separation by permeances of mixture components on 40 hollows fibers from polyetherimide with polyimide (Figure 6) is equal to 82.63 mol.% and by results of modeling by individual permeances - 82.12 mol.%. For oxygen, these values are 48.76 mol.% and 48.11 mol.%, respectively. The effective areas for the membrane modules made of polyetherimide and polyetherimide with polyimide are equal because they have the same diameters and are 36.2 cm^2.

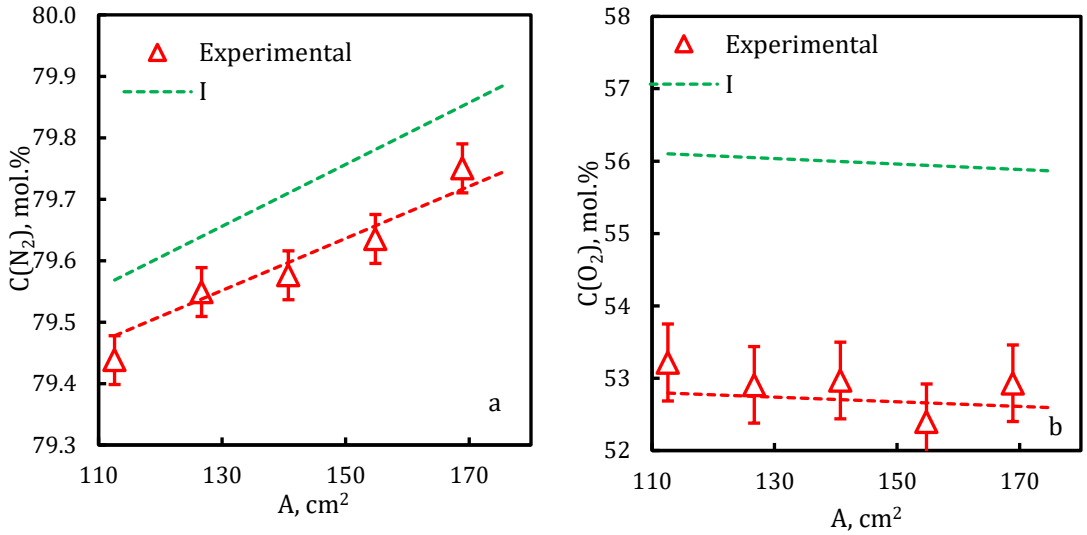

Figure 4 Dependence of concentration (a - N_2 in the retentate stream; b - O_2 in the permeate stream) on the effective area of the PPO membrane. Experimental - experimentally obtained concentrations of components; M - line obtained by modeling of the gas separation process considering the mixture gas transport characteristics; I - line obtained by modeling of the gas separation process taking into account the gas transport characteristics of individual components

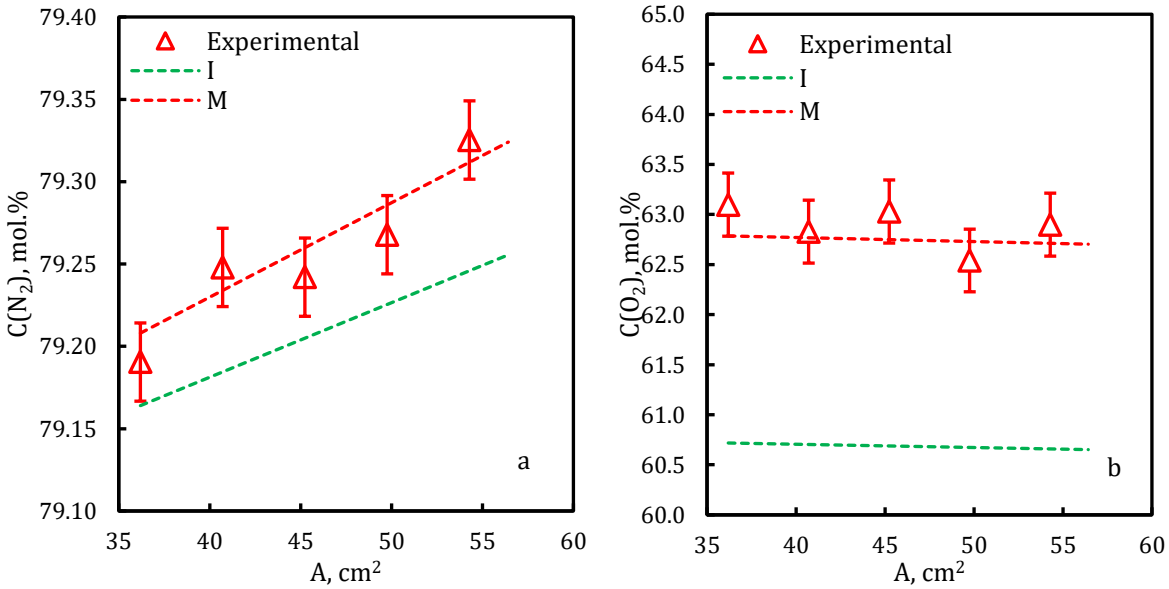

Figure 5 Dependence of concentration (a - N_2 in retentate stream; b - O_2 in permeate stream) on the effective area of PEI membrane. Experimental - experimentally obtained concentrations of components; M - line obtained by modeling of the gas separation process taking into account the mixture gas transport characteristics; I - line obtained by modeling of the gas separation process taking into account the gas transport characteristics of individual components

Experimental results for air separation confirmed the dependences described by the model constructed on the basis of gas transport characteristics obtained for the mixture.

The modeled lines plotted over a small stage-cut range are described by the following linear equations (see equations 5-20):

Polysulfone hollow fiber gas separation membrane:

For line I:

$$C(N_2)\ [mol.\%] = A\ [cm^2] * 0.0053 + 79; \quad (5)$$

$$C(O_2)\ [mol.\%] = A\ [cm^2] * (-0.0056) + 50.278; \quad (6)$$

For line M:

$$C(N_2)\ [mol.\%] = A\ [cm^2] * 0.0043 + 79; \quad (7)$$

$$C(O_2)\ [mol.\%] = A\ [cm^2] * (-0.0032) + 45.741. \quad (8)$$

Polyphenylene oxide hollow fiber gas separation membrane:
For line I:

$$C(N_2)\ [mol.\%] = A\ [cm^2] * 0.005 + 79.002; \quad (9)$$

$$C(O_2)\ [mol.\%] = A\ [cm^2] * (-0.0038) + 56.527; \quad (10)$$

For line M:

$$C(N_2)\ [mol.\%] = A\ [cm^2] * 0.0042 + 79.001; \quad (11)$$

$$C(O_2)\ [mol.\%] = A\ [cm^2] * (-0.0032) + 53.155. \quad (12)$$

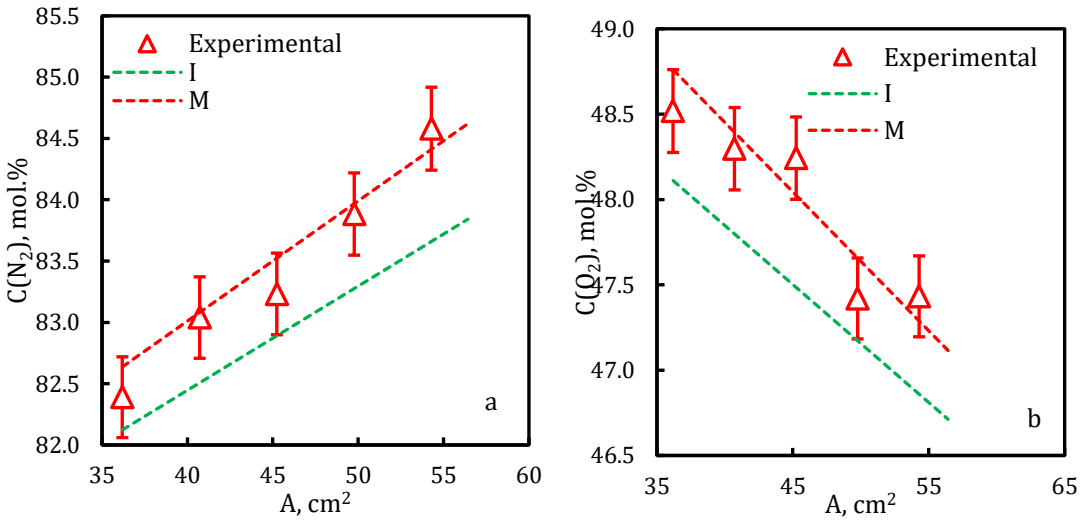

Figure 6 Dependence of concentration (a - N_2 in retentate stream; b - O_2 in permeate stream) on the effective area of PEI+PI membrane. Experimental - experimentally obtained concentrations of components; M - line obtained by modeling of the gas separation process taking into account the mixture gas transport characteristics; I - line obtained by modeling of the gas separation process taking into account the gas transport characteristics of individual components

Polyetherimide hollow fiber gas separation membrane:
For line I:

$$C(N_2)\ [mol.\%] = A\ [cm^2] * 0.0045 + 79; \quad (13)$$

$$C(O_2)\ [mol.\%] = A\ [cm^2] * (-0.0033) + 62.933; \quad (14)$$

For line M:

$$C(N_2)\ [mol.\%] = A\ [cm^2] * 0.0057 + 79; \quad (15)$$

$$C(O_2)\ [mol.\%] = A\ [cm^2] * (-0.0032) + 45.741. \quad (16)$$

Polyetherimide-polyimide hollow-fiber gas separation membrane:

For line I:

$$C(N_2)\ [mol.\%] = A\ [cm^2] * 0.0849 + 79.049; \quad (17)$$

$$C(O_2)\ [mol.\%] = A\ [cm^2] * (-0.0691) + 50.611; \quad (18)$$

For line M:

$$C(N_2)\ [mol.\%] = A\ [cm^2] * 0.098 + 79.091; \quad (19)$$

$$C(O_2)\ [mol.\%] = A\ [cm^2] * (-0.0813) + 51.704 \quad (20)$$

Then, the gas separation process was modeled for each membrane type over the whole stage-cut range. The modeled lines were supplemented with experimental data obtained during the separation of membrane modules. The graphs are presented in Figures 7-10.

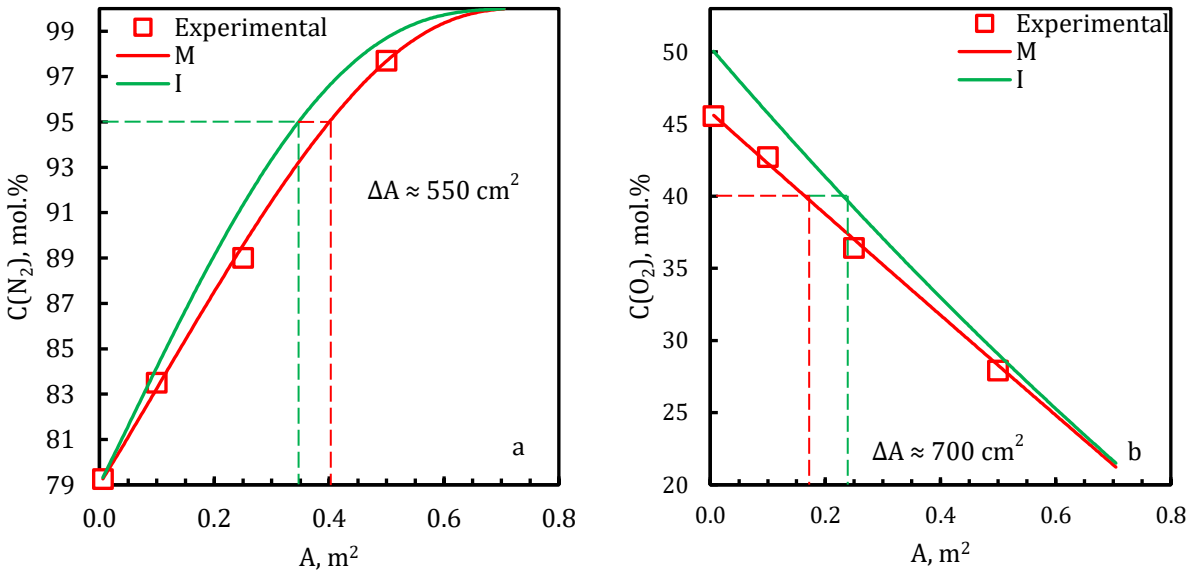

Figure 7 Dependence of concentration (a - N_2 in the retentate stream; b - O_2 in the permeate stream) on the effective area of the PSF membrane across the entire range of stage-cut. "Experimental" refers to the experimentally obtained concentrations of the components; "M" represents the line obtained by modeling the gas separation process considering the gas transport characteristics of the mixture; "I" represents the line obtained by modeling the gas separation process considering the gas transport characteristics of individual components

Figures 7-10 also show pairwise patterns. If to compare the graphs for nitrogen, for the pair polysulfone (Figure 7) and polyphenylene oxide (Figure 8) the line M passes under line I, and for the pair polyetherimide (Figure 9) and polyetherimide with polyimide (Figure 10) on the contrary - the line M passes above the line I, as it was noticed earlier in Figures 3-6.

A different dependence is observed for the plots with dependencies of oxygen concentration in the permeate stream on the effective area of the membrane. For PSF and PPO membranes, an increase in the effective area leads to the narrowing of the I and M lines and, eventually, their overlap. For PEI membranes, at a stage-cut value of 0.004 (membrane area 140 cm^2), the M line is higher than the I line; at a value of 0.01, the lines intersect and then invert so that for one effective area, the oxygen concentration in the permeate stream for the M line is lower than for the I line. And the larger the effective area, the more the calculated lines diverge. For the PEI+PI membrane, the same pattern with a crossover point at stage-cut 0.23 or an area of 84 cm^2.

The model lines were compared for nitrogen and oxygen concentrations of 95 mol.% and 40 mol.%, respectively. The divergence of the effective area results for each of the membranes is presented quantitatively in Figures 9-12 and as a percentage of area

deviation (A_{dif}) when calculating the mixture characterization data from the individual characterization data in Table 4.

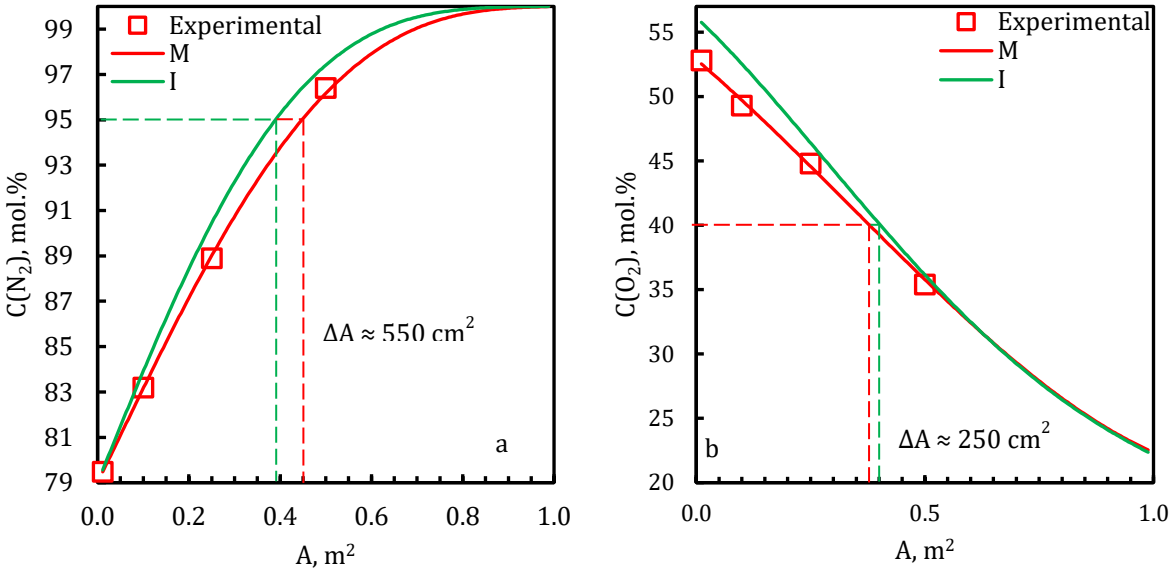

Figure 8 Dependence of concentration (a - N_2 in retentate stream; b - O_2 in permeate stream) on the effective area of PPO membrane in the whole range of stage-cut. Experimental - experimentally obtained concentrations of components; M - line obtained by modeling of the gas separation process taking into account the mixture gas transport characteristics; I - line obtained by modeling of the gas separation process considering the gas transport characteristics of individual components

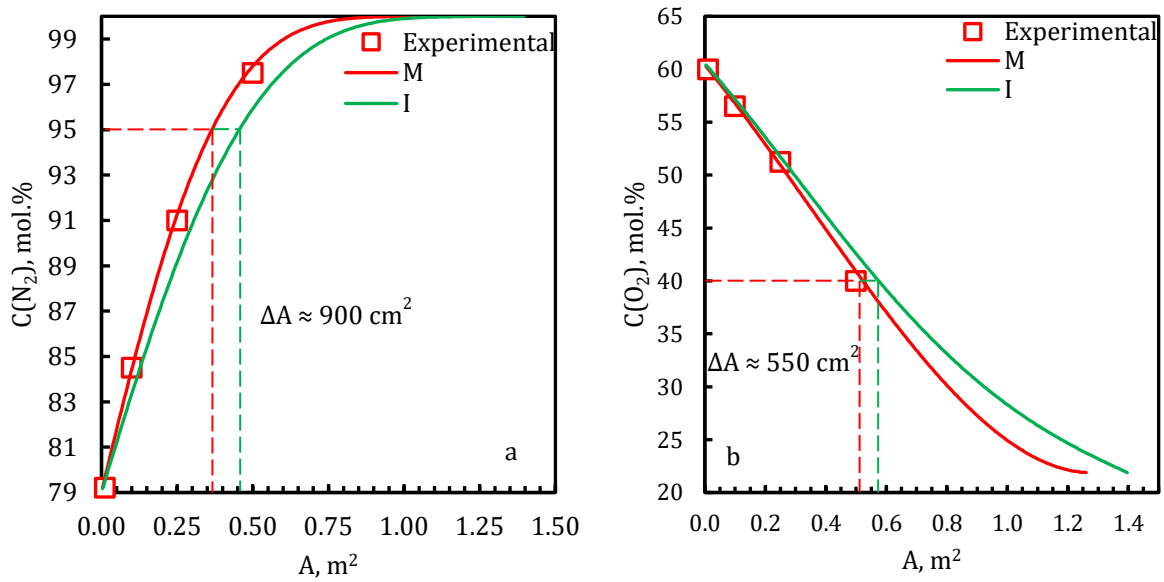

Figure 9 Dependence of concentration (a - N_2 in retentate stream; b - O_2 in permeate stream) on the effective area of PEI membrane in the whole range of stage-cut. Experimental - experimentally obtained concentrations of components; M - line obtained by modeling of the gas separation process taking into account the mixture gas transport characteristics; I - line obtained by modeling of the gas separation process considering the gas transport characteristics of individual components

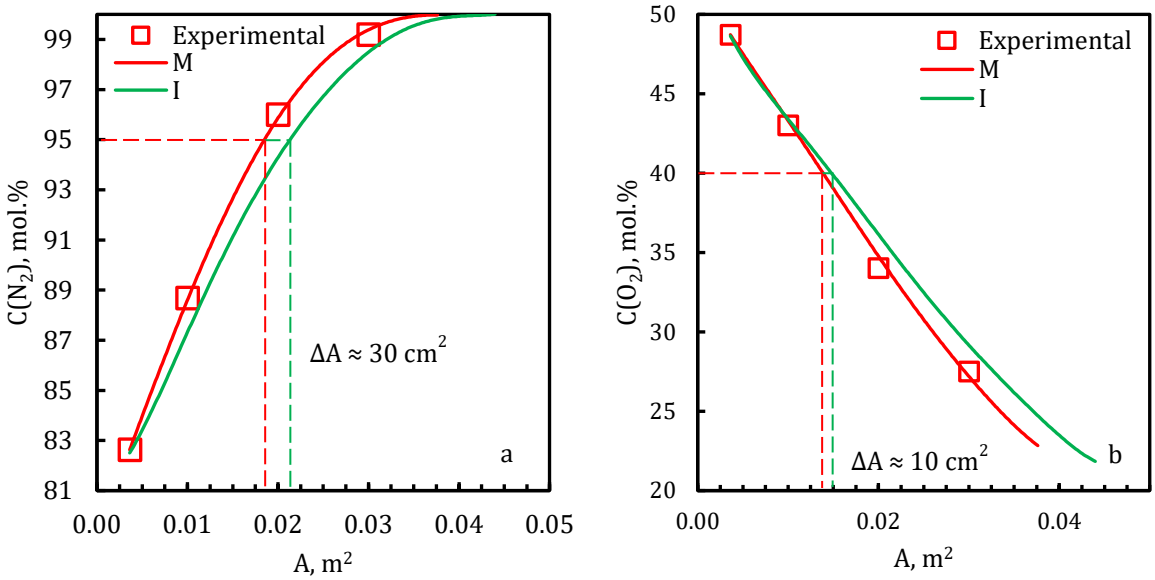

Figure 10 Dependence of concentration (a - N_2 in retentate stream; b - O_2 in permeate stream) on the effective area of PEI+PI membrane in the whole range of stage-cut. Experimental - experimentally obtained concentrations of components; M - line obtained by modeling of the gas separation process taking into account the mixture gas transport characteristics; I - line obtained by modeling of the gas separation process considering the gas transport characteristics of individual components

$$A_{dif} = \frac{|A_m - A_i|}{A_i} \times 100\ \%, \quad (21)$$

where A_m – membrane area is calculated taking into account the mixture characteristics, cm²; A_i – membrane area is calculated taking into account the characteristics obtained during the permeance study of individual gases, cm².

Table 4 Deviations of effective membrane areas required to achieve a nitrogen concentration in the retentate stream of 95 mol.% and an oxygen concentration in the permeate stream of 40 mol.%

Membrane	A_{dif}, % (N_2)	A_{dif}, % (O_2)
PSF	15.8	29.2
PPO	13.9	6.25
PEI	19.8	9.7
PEI+PI	15.9	6.7

According to the data presented in Table 3, when designing a membrane gas separator with a polysulfone hollow fiber membrane based on the permeances of the individual components of nitrogen and oxygen, a larger number of membranes will be required to achieve the required nitrogen concentration. For example, to achieve a concentration of 95 mol.% nitrogen, increasing the effective membrane area by 15.8 % would be necessary. For the oxygen extraction task, the situation would be the opposite, and the calculated quantity would be 29.2 % more than required, which could lead to unnecessary manufacturing costs. For polyphenylene oxide membranes, a similar relationship holds. Membranes made of polyetherimide and polyetherimide with polyimide, both for oxygen and nitrogen extraction tasks, demonstrate that the calculated amount will be in excess. Thus, 19.8 % less membrane is needed for nitrogen extraction than calculated for the polyimide membrane.

4. Conclusions

In the present work, the gas transport characteristics of hollow fiber gas separation membranes made of PSF, PPO, PEI, and PEI+PI have been investigated. Two series of measurements were carried out; permeance values were obtained for individual components of the gas mixture, as well as for the separation of a real air-gas mixture. Based on the obtained results, we carried out mathematical modeling of the gas separation process in the membrane cell. Our findings demonstrate that the modeling, which relied on the permeance values for individual gases, has significant discrepancies with the data on the separation of an air-gas mixture. The data shows a significant discrepancy of 20 percent or more in the values. The main expense item in membrane gas separation processes are compressor stations, the required capacity of which is directly related to the number of membrane modules and membrane elements. An error in calculating the effective membrane area when designing installations will lead to significant capital and operating costs. In one case, such errors will lead to the purchase of expensive equipment of excessive capacity, in the other to the fact that the calculated capacity will not be sufficient to achieve the planned indicators. From the fundamental side, the permeability values of commercially available membranes for air-gas mixture separation tasks are presented. Thus, when modeling membrane gas separation plants, cascades, and production facilities, there is a need to study specifically the mixture gas transport characteristics - permeance values obtained by analyzing the flows through the membrane of each individual component of the gas mixture.

Acknowledgments

The main part of the work was carried out with financial support from the Ministry of Science and Higher Education of the Russian Federation within the framework of a scientific project under state assignment No. FSSM-2023-0004. The study of the permeances of pure gases was carried out with the support of the Government of the Tula Region, agreement No. 14 of September 14, 2023.

Conflict of Interest

The authors declare no conflicts of interest.

References

Atlaskin, A.A., Trubyanov, M.M., Yanbikov, N.R., Kryuchkov, S.S., Chadov, A.A., Smorodin, K.A., Drozdov, P.N., Vorotyntsev, V.M., Vorotyntsev, I.V., 2020. Experimental Evaluation of the Efficiency of Membrane Cascades Type of “Continuous Membrane Column” in the Carbon Dioxide Capture Applications. *Membranes and Membrane Technologies*, Volume 2, pp. 35–44

Atlaskin, A.A., Trubyanov, M.M., Yanbikov, N.R., Vorotyntsev, A. V., Drozdov, P.N., Vorotyntsev, V.M., Vorotyntsev, I.V., 2019. Comprehensive Experimental Study of Membrane Cascades Type Of “Continuous Membrane Column” For Gases High-Purification. *Journal of Membrane Science,* Volume 572, pp. 92–101

Barbari, T.A., Koros, W.J., Paul, D.R., 1989. Polymeric Membranes Based on Bisphenol-A For Gas Separations. *Journal of Membrane Science,* Volume 42, pp. 69–86

Bera, S.P., Godhaniya, M., Kothari, C., 2022. Emerging and Advanced Membrane Technology For Wastewater Treatment: A Review. *Journal of Basic Microbiology,* Volume 62, pp. 245–259

Bittner, K., Margaritis, N., Schulze-Küppers, F., Wolters, J., Natour, G., 2023. A Mathematical

Model for Initial Design Iterations and Feasibility Studies of Oxygen Membrane Reactors By Minimizing Gibbs Free Energy. *Journal of Membrane Science,* Volume 685, p. 121955

Checchetto, R., Scarpa, M., De Angelis, M.G., Minelli, M., 2022. Mixed Gas Diffusion And Permeation Of Ternary and Quaternary CO2/CO/N2/O2 Gas Mixtures in Matrimid®, Polyetherimide and Poly(Lactic Acid) Membranes for CO2/CO Separation. *Journal of Membrane Science,* Volume 659, p. 120768

Chen, X.Y., Kaliaguine, S., Rodrigue, D., 2019. Polymer Hollow Fiber Membranes For Gas Separation: A Comparison Between Three Commercial Resins. In: AIP Conference Proceedings, Volume 2139(1), p. 070003

Chenar, M.P., Soltanieh, M., Matsuura, T., Tabe-Mohammadi, A., Feng, C., 2006. Gas Permeation Properties of Commercial Polyphenylene Oxide and Cardo-Type Polyimide Hollow Fiber Membranes*. Separation and Purification Technology*, Volume 51, pp. 359–366

Cheng, M., Verma, P., Yang, Z., Axelbaum, R.L., 2021. Single-Column Cryogenic Air Separation: Enabling Efficient Oxygen Production With Rapid Startup and Low Capital Costs—Application To Low-Carbon Fossil-Fuel Plants. *Energy Conversion and Management,* Volume 248, p. 114773

Cheun, J. Y., Liew, J.Y.L., Tan, Q.Y., Chong, J.W., Ooi, J., Chemmangattuvalappil, N.G., 2023. Design of Polymeric Membranes for Air Separation by Combining Machine Learning Tools with Computer Aided Molecular Design. *Processes,* Volume 11, p. 2004

Chuah, C.Y., Goh, K., Bae, T.H., 2021. Enhanced Performance Of Carbon Molecular Sieve Membranes Incorporating Zeolite Nanocrystals For Air Separation. *Membranes,* Volume 11(7), p. 489

Du, N., Robertson, G.P., Dal-Cin, M.M., Scoles, L., Guiver, M.D., 2012. Polymers of Intrinsic Microporosity (PIMs) Substituted with Methyl Tetrazole. *Polymer,* Volume 53, pp. 4367–4372

Ekiner, O. M., Kulkarni, S.S., 2003. *U.S. Patent No. 6,663,805*. Washington, DC: U.S. Patent and Trademark Office

Fujikawa, S., Selyanchyn, R., Kunitake, T., 2020. A New Strategy For Membrane-Based Direct Air Capture. *Polymer Journal,* Volume 53(1), pp. 111–119

Hao, L., Li, P., Chung, T.S., 2014. PIM-1 as an Organic Filler To Enhance The Gas Separation Performance of Ultem Polyetherimide. *Journal of Membrane Science,* Volume 453, pp. 614–623

Ilyushin, Y.V., Kapostey, E.I., 2023. Developing a Comprehensive Mathematical Model for Aluminium Production in a Soderberg Electrolyser. *Energies*, Volume 16, p. 6313

Kamin, Z., Bahrun, M.H.V., Bono, A., 2022. A Short Review on Pressure Swing Adsorption (PSA) Technology for Nitrogen Generation from Air. *In:* AIP Conference Proceedings, Volume 2610, p. 050006

Karamah, E.F., Arbi, D.S., Bagas, I., Kartohardjono, S., 2021. Hollow Fiber Membrane Modules for NOx Removal using a Mixture of NaClO3 and NaOH Solutions in the Shell Side as Absorbents. *International Journal of Technology,* Volume 12(4), pp. 690–699

Kartohardjono, S., Karamah, E.F., Hayati, A.P., Talenta, G.N., Ghazali, T.A., Lau, W.J., 2024. Effect of Oxidants in the Utilization of Polysulfone Hollow Fiber Membrane Module as Bubble Reactor for Simultaneously Removal of NOx and SO2 . *International Journal of Technology,* Volume 15(1), pp. 63–74

Kartohardjono, S., Karamah, E.F., Talenta, G.N., Ghazali, T.A., Lau, W.J., 2023. The Simultaneously Removal of NOx and SO2 Processes through a Polysulfone Hollow Fiber Membrane Module. *International Journal of Technology*, Volume 14(3), pp. 576–

583
Kianfar, E., Cao, V., 2021. Polymeric Membranes on Base of Polymethyl Methacrylate for Air Separation: A Review. *Journal of Materials Research and Technology*, Volume 10, pp. 1437–1461
Krzystowczyk, E., Haribal, V., Dou, J., Li, F., 2021. Chemical Looping Air Separation Using a Perovskite-Based Oxygen Sorbent: System Design and Process Analysis. *ACS Sustainable Chemistry & Engineering,* Volume 9, pp. 12185–1219501
Liu, K.G., Bigdeli, F., Panjehpour, A., Hwa Jhung, S., Al Lawati, H.A.J., Morsali, A., 2023. Potential Applications of MOF Composites as Selective Membranes for Separation of Gases. *Coordination Chemistry Reviews,* Volume 496, p. 215413
Mayer, M.J., Gróf, G., 2020. Techno-Economic Optimization of Grid-Connected, Ground-Mounted Photovoltaic Power Plants By Genetic Algorithm Based on A Comprehensive Mathematical Model. *Solar Energy*, Volume 202, pp. 210–226
Ng, B.C., Ismail, A.F., Rahman, W.A., Hasbullah, H., Abdullah, M.S., Hassan, A.R., 2004. Formation of Asymmetric Polysulfone Flat Sheet Membrane 73 Formation Of Asymmetric Polysulfone Flat Sheet Membrane For Gas Separation: Rheological Assessment. Jurnal Teknologi, Volume 41, pp. 73–88
Petukhov, A.N., Atlaskin, A.A., Kryuchkov, S.S., Smorodin, K.A., Zarubin, D.M., Petukhova, A.N., Atlaskina, M.E., Nyuchev, A.V., Vorotyntsev, A.V., Trubyanov, M.M., Vorotyntsev, I. V., Vorotynstev, V.M., 2021. A Highly-Efficient Hybrid Technique – Membrane-Assisted Gas Absorption For Ammonia Recovery after the Haber-Bosch Process. *Chemical Engineering Journal,* Volume 421, p. 127726
Petukhov, A.N., Shablykin, D.N., Trubyanov, M.M., Atlaskin, A.A., Zarubin, D.M., Vorotyntsev, A. V., Stepanova, E.A., Smorodin, K.A., Kazarina, O. V., Petukhova, A.N., Vorotyntsev, V.M., Vorotynstev, I.V., 2022. A Hybrid Batch Distillation/Membrane Process For High Purification Part 2: Removing Of Heavy Impurities From Xenon Extracted From Natural Gas. *Separation and Purification Technology,* Volume 294, p. 121230
Pfromm, P.H., Pinnau, I., Koros, W.J., 1993. Gas Transport Through Integral-Asymmetric Membranes: A Comparison To Isotropic Film Transport Properties. *Journal of Applied Polymer Science,* Volume 48(12), pp. 2161–2171
Pinnau, I., Koros, W.J., 1991. Structures and Gas Separation Properties of Asymmetric Polysulfone Membranes Made by Dry, Wet, And Dry/Wet Phase Inversion. *Journal of Applied Polymer Science,* Volume 43, pp. 1491–1502
Polotskaya, C.A., Agranova, S.A., Gazdina, N. V, Kuznetsov, Y.P., Nesterov, V. V, 1996. Effect of Molecular Weight Parameters on Gas Transport Properties of Poly(2,6-dimethyl-1,4-phenylene oxide). *Journal of Applied Polymer Science*, Volume 62(13), pp. 2215–2218
Polotskaya, G.A., Penkova, A. V., Toikka, A.M., Pientka, Z., Brozova, L., Bleha, M., 2007. Transport of Small Molecules through Polyphenylene Oxide Membranes Modified by Fullerene. *Separation Science and Technology,* Volume 42, pp, 333–347
Reid, B.D., Ruiz-Trevino, A., Musselman, I.H., Balkus, K.J., Ferraris, J.P., 2001. Gas Permeability Properties of Polysulfone Membranes Containing the Mesoporous Molecular Sieve MCM-41. *Chemistry of Materials,* Volume 13(7), pp. 2366–2373
Saimani, S., Kumar, A., Dal-Cin, M.M., Robertson, G., 2011. Synthesis and Characterization of Bis (4-maleimidophenyl) Fluorene and its Semi Interpenetrating Network Membranes with Polyether Imide (Ultem® 1000*). Journal of Membrane Science,* Volume 374, pp. 102–109
Thomas, S., Pinnau, I., Du, N., Guiver, M.D., 2009. Hydrocarbon/Hydrogen Mixed-Gas Permeation Properties of PIM-1, An Amorphous Microporous Spirobisindane Polymer.

Journal of Membrane Science, Volume 338, pp. 1–4

Tian, T., Wang, Y., Liu, B., Ding, Z., Xu, X., Shi, M., Ma, J., Zhang, Y., Zhang, D., 2022. Simulation and Experiment of Six-Bed PSA Process for Air Separation With Rotating Distribution Valve. *Chinese Journal of Chemical Engineering,* Volume 42, pp. 329–337

Trubyanov, M.M., Kirillov, S.Y., Vorotyntsev, A.V., Sazanova, T.S., Atlaskin, A.A., Petukhov, A.N., Kirillov, Y.P., Vorotyntsev, I.V., 2019. Dynamic Behavior of Unsteady-State Membrane Gas Separation: Modelling of a Closed-Mode Operation for a Membrane Module. *Journal of Membrane Science,* Volume 587, p. 117173

Tu, Y., Zeng, Y., 2021. Experimental Study on the Performance of an Onboard Hollow-Fiber-Membrane Air Separation Module. *Fluid Dynamics & Materials Processing,* Volume 18, pp. 355–370

Valappil, R.S.K., Ghasem, N., Al-Marzouqi, M., 2021. Current and Future Trends in Polymer Membrane-Based Gas Separation Technology: A Comprehensive Review. *Journal of Industrial and Engineering Chemistry*, Volume 98, pp. 103–129

Visser, T., Masetto, N., Wessling, M., 2007. Materials Dependence of Mixed Gas Plasticization Behavior in Asymmetric Membranes. *Journal of Membrane Science,* Volume 306, pp. 16–28

Vorotyntsev, V.M., Drozdov, P.N., Vorotyntsev, I.V., Murav'Ev, D.V., 2006. Fine Gas Purification To Remove Slightly Penetrating Impurities Using a Membrane Module With a Feed Reservoir. *Doklady Chemistry*, Volume 411, pp. 243–245

Wright, C.T., Paul, D.R., 1998. Gas Sorption and Transport in UV-Irradiated Poly(2,6-dimethyl-1,4-phenylene oxide) Films*. Journal of Applied Polymer Science,* Volume 67(5), pp. 875–883

Young, A.F., Villardi, H.G.D., Araujo, L.S., Raptopoulos, L.S.C., Dutra, M.S., 2021. Detailed Design and Economic Evaluation of a Cryogenic Air Separation Unit with Recent Literature Solutions. *Industrial & Engineering Chemistry Research*, Volume 60, pp. 14830–14844

Zhou, X., Rong, Y., Fang, S., Wang, K., Zhi, X., Qiu, L., Chi, X., 2021. Thermodynamic Analysis of an Organic Rankine–Vapor Compression Cycle (ORVC) Assisted Air Compression System for Cryogenic Air Separation Units. *Applied Thermal Engineering,* Volume 189, p. 116678